

Preparation and Physical Properties of EuO Nanocrystals Using Eu(II)-Exchanged Zeolite X as a Precursor

Supitcha Thongchant, Shinya Katagiri, Yasuchika Hasegawa, Yuji Wada,[1] Seiji Watase,[1] Masami Nakamoto,[2] Takao Sakata,[2] Hirotaro Mori, and Shozo Yanagida*

Material and Life Science, Graduate School of Engineering, Osaka University, 2-1, Yamadaoka, Suita, Osaka 565-0871

[1]Osaka Municipal Technical Research Institute, Morinomiya, Joto-ku, Osaka 536-8553

[2]Research Center for Ultra-High Voltage Electron Microscopy, Osaka University, 2-1, Yamadaoka, Suita, Osaka 565-0871

Received June 9, 2003; E-mail: yanagida@mls.eng.osaka-u.ac.jp

The cation-exchange of zeolite X with divalent europium has been achieved using a methanol solution containing Eu(II) prepared by photochemical reduction of Eu(III). Emission spectra have confirmed that the valence of europium ion in the ion-exchanged zeolite X was divalent. A blue shift of emission spectra was observed after exposing Eu(II)X to air at room temperature. TEM have revealed the formation of EuO nanocrystals with average size of 4.2 nm on the outer surface of Eu(II)X. EuO nanocrystals show ferromagnetism accompanied by photo-response magnetism under UV irradiation.

Zeolite is known as a useful nano-scaled host for functional organic molecules, semiconductors and metals since it has well-defined crystal structure with an internal porous open framework of molecular dimension.[1–16] Lately, new approaches using the cavity of zeolite for a host of an emitting center have been demonstrated, in which the Nd(III) complex and the Eu(III) complexes in a supercage of faujasite-typed zeolite showed highly efficient luminescence from 4f–4f electronic transition.[5–9]

On the other hand, the electronic transition of Eu(II) is assigned to 4f–5d allowed transition, and leads to the broad emission and optomagnetic properties. An oxide form of Eu(II), i.e., EuO, is a ferromagnetic semiconductor.[17] Especially, the nanocrystals of EuO and EuS show photoemission and magnetic properties that are different from those of bulk compounds.[18–23] Although Eu(II)-containing zeolites have high potential as luminescent and optomagnetic materials, only a few reports by Stucky and Arakawa have described Eu(II)-containing zeolites.[24–28] Arakawa and co-workers reported that Eu(III) in Y-type zeolite could be reduced to Eu(II) upon heat-treatment above 300 °C.[26–28] However, it contained only a little amount of Eu(II) cations per unit cell.

Zeolite X can contain a high density of cations per unit cell because of a large supercage size (13 Å) and ease of ion exchange. In 1980s, Stucky and co-workers reported that in the ion exchange reaction of zeolites with $Eu(OH)_2 \cdot (H_2O)_x$, the zeolites involved Eu(III) instead of Eu(II) because of the instability of $Eu(OH)_2 \cdot (H_2O)_x$.[24,25] They also introduced Eu(II) into A, Y, and X zeolites by ion exchange reaction via metallic europium dissolved in liquid ammonia.[24,25] According to their reports, the metal in liquid ammonia gave defects in zeolites that affected the physical properties of the samples.

In this work, we have successfully introduced Eu(II) into zeolite X through ion-exchange reaction using a Eu(II) solution prepared by a photochemical reaction for the first time. Europium(II) cations in zeolite X were characterized by ICP-AES (Inductively Coupled Plasma Atomic Emission Spectroscopy), XPS (X-ray Photoelectron Spectroscopy) and photoemission spectra. Furthermore, by oxidation of Eu(II)X in the atmosphere, we have found that EuO nanocrystals were formed on the outer surface of zeolite X. The optical, magnetic and photo-response magnetic properties of the EuO nanocrystals on the surface of zeolite are discussed using fluorescent spectra and magnetic measurements.

Experimental

Materials. Europium(III) chloride ($EuCl_3 \cdot 6H_2O$ 99.99%), methanol (CH_3OH 99.99%), potassium carbonate (K_2CO_3 99.5%) and the standard europium and aluminum solutions (1000 ppm) were purchased from Wako Pure Chemical Industries, Ltd. Zeolite Na-13X with composition of $Na_{86}(AlO_2)_{86}(SiO_2)_{106} \cdot 26H_2O$ was bought from Nikka-Seiko Co., Ltd. All of the chemicals were reagent grade and were used as received.

Preparation of Eu(II)Cl_2 Solution. In a quartz vessel, $EuCl_3$ (75 mM) was dissolved in methanol (200 mL), and the solution was irradiated by a low-pressure mercury arc lamp (200 W) at 25 °C under an inert atmosphere. The reduction reaction of Eu(III) to Eu(II) was monitored by the emission of Eu(II) and Eu(III) at 425 nm and 475 nm, respectively. The complete reaction took 8 days.

Ion Exchange Reaction. Europium(II)-Exchanged Zeolite X (Eu(II)X): Under an inert atmosphere, Na-exchanged zeolite X (NaX) (1.0 g) was added to a methanol solution of Eu(II)Cl_2 (75 mM, 100 mL) and stirred at room temperature for 48 h. The zeolite X was washed several times with pure methanol. The powder was introduced into a quartz optical cell, then heat-dried (120 °C, 2 h) and closed in vacuum. The obtained sample was pale

Published on the web April 2, 2004; DOI 10.1246/bcsj.77.807

yellow powder.

Europium(III)-Exchanged Zeolite X (Eu(III)X): Sodium-exchanged zeolite X (NaX) (1.0 g) was added to water solution of $Eu(III)Cl_3$ (75 mmol, 100 mL) and refluxed for 24 h. The zeolite was washed with de-ionized water several times. The powder was introduced to a quartz optical cell, then heat-dried (120 °C, 2 h) and closed in vacuum. The obtained sample was white powder.

Preparation of EuO Nanocrystals from Eu(II)X (Eu(II)X-air). The Eu(II)X was kept in the atmosphere at room temperature for 24 h. The sample after being exposed to air is named 'Eu(II)X-air'. After being exposed to air, the sample was kept in inert gas for further characterization. Eu(II)X-air was characterized by transmission electron microscopy (TEM), the electron diffraction patterns and magnetic measurements. A small amount of Eu(II)X-air was kept in atmosphere and its emission spectra were monitored.

Apparatus. Inductively Coupled Plasma Atomic Emission Spectroscopy (ICP-AES) analysis was performed on a Seiko Instruments SPS1500VR. Europium(II)-exchanged zeolite X (Eu(II)X) or Eu(III)X was mixed with K_2CO_3 powder and heated until the mixture was turned into a melting salt. The samples were diluted with 1 M HNO_3 solution. The standard solution was prepared from commercially available 1000 ppm Eu and Al standard stock solutions, respectively. The ion exchange level was calculated using the molar ratio of aluminum and europium as shown in Eq. 1.

$$\text{Ion exchange level (\%)} = (\text{Eu (mol)} \times n/\text{Al (mol)} \times 1) \times 100$$
(n: valence number; $n = 2$ for Eu(II)X, $n = 3$ for Eu(III)X) (1)

X-ray diffraction (XRD) patterns were recorded on a Rigaku X-ray Diffractometer Multiflex using monochromated Cu Kα radiation. No significant difference of XRD patterns was observed after the ion exchange of NaX with Eu(II) and Eu(III).

Transmission Electron Microscopy (TEM) images were obtained with a Hitachi H-9000 TEM equipped with a tilting device ($\pm$10 degrees) and operating at 300 kV ($C_s = 0.9$ nm). Images were recorded under axial illumination at approximate Scherzer focus, with a point resolution better than 0.9 nm.

The photoemission spectra of $EuCl_3$ solution, Eu(II)X, Eu(III)X, and Eu(II)X-air powder samples were measured by a Hitachi F-4500 fluorescent spectrophotometer at room temperature.

X-ray Photoelectron Spectroscopy (XPS) spectra were recorded on PHI ESCA5700 using monochromated Al Kα radiation (1486.6 eV) at 350 W (14.0 KV, 35 mA). A base pressure of 1.0×10^{-9} Torr was maintained during the experiments. Europium(II)-exchanged zeolite X (Eu(II)X) or Eu(III)X power was ground with a small amount of boron nitride (BN, B1s: 190.5 eV) as the internal standard and pressed into a pellet to give a circular disk <0.5 mm thickness and 5 mm in diameter. The B1s line (190.5 eV) of the internal standard was used for spectral calibration. Before the measurements, the surfaces of the samples were carefully cleaned by Ar^+ beam (4 kV) for 2 min.

Magnetic measurements were performed by a superconducting quantum interference device (SQUID) magnetometer. Each sample was pressed into a small disk having the thickness of less than 0.5 mm and the area of 2×3 mm^2. The correlation between magnetization and temperature was recorded under magnetic field at 0.1 T, for temperatures from 10 to 150 K. The correlation between magnetization and magnetic field was recorded at 5 K under magnetic fields from -1.0 to 1.0 T with and without irradiation by a low-pressure mercury arc lamp ($\lambda = 254$ nm) via an optical fiber.

$$Eu^{III}(CH_3OH])_n + h\nu \longrightarrow Eu^{II}(CH_3OH)_{n-1} + CH_3OH^+$$
$$CH_3OH^+ + CH_3OH \longrightarrow CH_3OH_2^+ + \cdot CH_2OH$$
$$\cdot CH_2OH + Eu(III) \longrightarrow Eu(II) + H^+ + HCHO$$

Scheme 1. Photochemical reduction of Eu(III) to Eu(II).

Results and Discussion

Preparation of Eu(II)X and Eu(III)X. Commonly, Eu(II) is oxidized into Eu(III) rapidly with oxygen and moisture in the atmosphere. For example, the ion exchange reaction of zeolites with $Eu(OH)_2 \cdot (H_2O)_x$, gives Eu(III) instead of Eu(II) in the zeolites because of the instability of $Eu(OH)_2 \cdot (H_2O)_x$.[24,25] The commercially available $EuCl_2$ is not stable enough for the long-time ion exchange reaction. We performed the ion exchange of NaX with the Eu(II) solution prepared by the photoreduction of $EuCl_3$ in methanol. As the result we obtained the first Eu(II)-exchanged zeolite which was stable in inert gas. The photoreductions of Eu(III) to Eu(II) were previously reported by Donohou,[29,30] and by Kusaba and co-workers.[31] The reaction is shown in Scheme 1. In our previous work, we reported that, in photochemical synthesis of EuO nanocrystals, formaldehyde reacts with urea to give polyurea, which stabilizes the surface of EuO nanocrystals.[21] In this case, organic molecules generated in the later steps ($(HCHO)_n$, HCOOH, etc.) are considered to be stabilizers for Eu(II) in methanol.

Characterization of Eu(II) in Eu(II)X. The reduction process of Eu(III) to Eu(II) was monitored by the emission spectra of the europium ions. Eu(III) showed a sharp red emission spectrum at 613 nm due to $^5D_0 \rightarrow {}^7F_2$ electronic transition, and Eu(II) showed a broad emission due to the 4f–5d electron transition. Upon the irradiation of UV light to a methanol solution of $EuCl_3$, the emission intensity of Eu(III) at 613 nm decreased gradually (Fig. 1a). In contrast, the emission intensity of Eu(II) at 425 nm increased (Fig. 1b). These results indicated that Eu(III) was reduced into Eu(II) under UV irradiation. A valley-shaped decrease around 395 nm in the emission spectra was attributed to the absorption of Eu(III) ($^7F_0 \rightarrow {}^5L_6$). Europium(II)-exchanged zeolite X (Eu(II)X) was prepared by the ion exchange reaction of zeolite NaX with the above Eu(II) methanol solution.

Figure 1c shows the emission spectra of $EuCl_2$ in methanol and Eu(II)X under excitation at 360 nm. The peak top of the band emission shifted from 425 to 475 nm in the emission of Eu(II)X. Europium(II) was thought to be successfully introduced into the cavity of zeolite X because the shift of the emission was caused by the change in the environment from a methanol solution to the cavity of zeolite X. Note that the reported emission of Eu(II) in zeolite Y and mordenite was observed at 455 nm and 488 nm, respectively.[26–28] On the other hand, we observed only a line emission of Eu(III) at 613 nm from Eu(III)X.

The compositions of Eu(II)X and Eu(III)X determined by ICP-AES are shown in Table 1. The ion exchanged degree of Eu(II)X and Eu(III)X were 54% and 95%, respectively. While the ion exchange level of Eu(II)X was lower than Eu(III)X because of the difference in their valence numbers, the numbers of europium ions per unit cell for Eu(II)X and Eu(III)X were estimated to be 23 and 27, respectively.

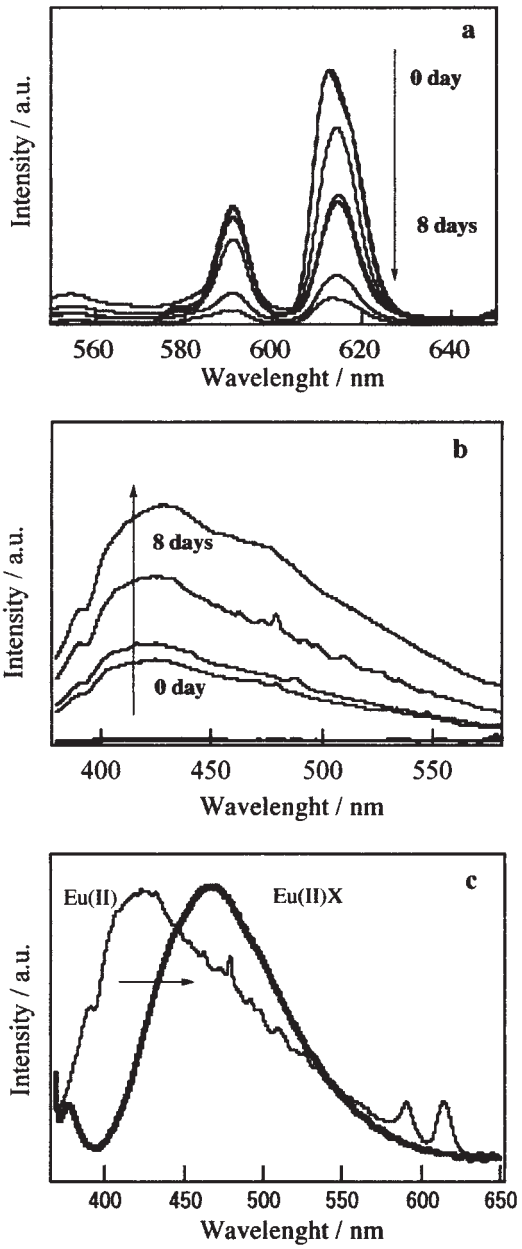

Fig. 1. (a) Emission spectra of Eu(III) in the reaction solution from 0 to 8 days (Ex = 395 nm). (b) Emission spectra of Eu(II) in the reaction solution from 0 to 8 days (Ex = 360 nm). (c) The emission spectrum of the reaction solution at the 8th day compared with that of Eu(II)X (Ex = 360 nm).

Table 1. Ratio of Europium and Aluminum and Ion Exchange Levels in Eu(II)X and Eu(III)X Determined by ICP-AES

Samples	Eu(II)X	Eu(III)X
Al (ppm/mmol)	17.76/0.66	103.842/3.85
Eu (ppm/mmol)	27.27/0.18	185.667/1.22
Exchange level/%	54	95
Number of Eu per unit cell	23.25	27.30

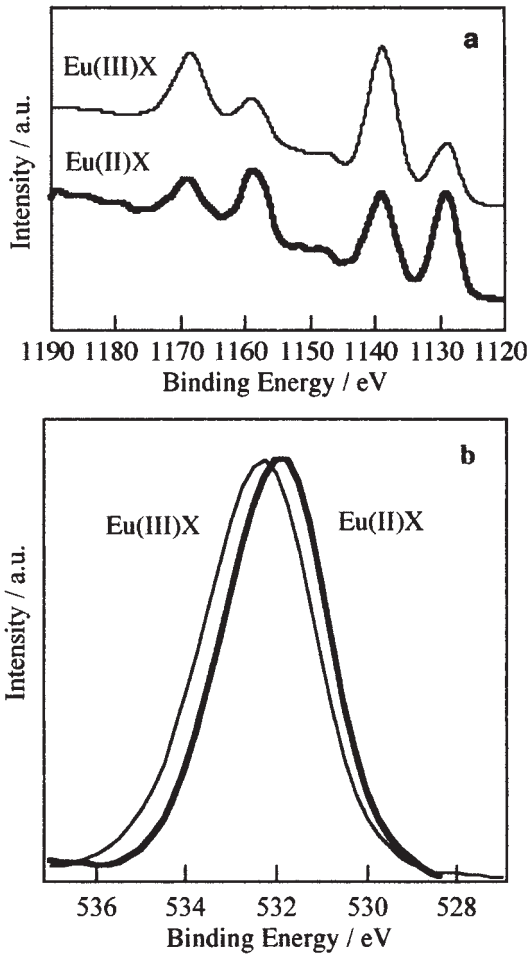

Fig. 2. (a) XPS spectra showing binding energy of Eu3d orbital in Eu(III)X and Eu(II)X. (b) XPS spectra showing binding energy of O1s orbital of Eu(III)X and Eu(II)X.

XPS analysis is a good tool to obtain the information of electronic states of the compounds.[32–34] The Eu3d spectra of Eu(II)X and Eu(III)X are shown in Fig. 2a. Compared with the binding energy of Eu(III)X, that of Eu(II)X revealed no shift. However, the shapes of the spectra were apparently different from each other. In the case of Eu(III)X, the peak intensity at 1159 eV and 1129 eV were smaller than those of 1169 eV and 1139 eV. On the other hand, the peak intensities at 1159 eV and 1129 eV of Eu(II)X were larger than those of at 1169 eV and 1139 eV. The result agreed with a previous report that the ratios between the satellite peaks and the main peaks of Eu3d of Eu(II) compounds were larger than those of Eu(III) compounds.[32–34] On the other hand, the difference between the interactions of framework oxygen and europium ion, i.e., O^{2-}/Eu(II) and O^{2-}/Eu(III) in zeolite X, was observed from the binding energy of O1s. The peak of O1s showed a shift by 0.7 eV from 531.7 eV of Eu(II)X to 532.5 eV of Eu(III)X (Fig. 2b), supporting the conclusion that Eu(II) and Eu(III) were incorporated in the zeolite.

Formation of EuO Nanocrystals from Eu(II)X. The changes of the emission spectra after exposing Eu(II)X to air (Eu(II)X-air) are shown in Fig. 3a. We observed that the intensity of the emission decreased, and the peak shifted toward shorter wavelength after 12 days-exposure to air (Fig. 3b).

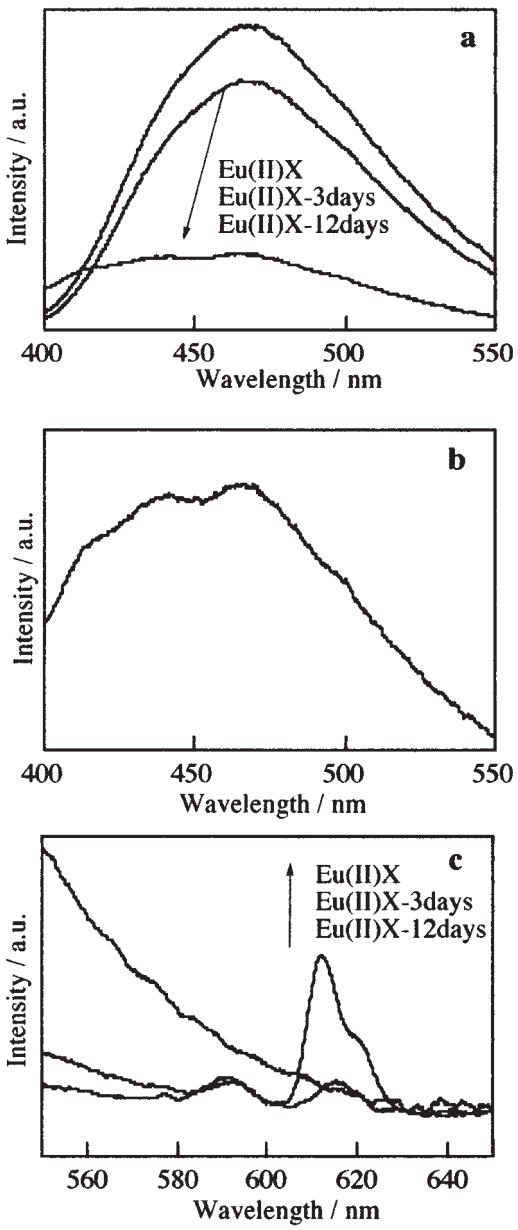

Fig. 3. (a) Change of the emission spectra of Eu(II)X in air (Ex = 360 nm). (b) Emission of Eu(II)X after 12 days (magnified). (c) Change of emission spectra of Eu(II)X in air (Ex = 395 nm).

The emission of Eu(III) gradually increased (Fig. 3c) in parallel. TEM images of Eu(II)X and Eu(II)X-air are shown in Figs. 4a–4e. The TEM image of Eu(II)X (Fig. 4b) showed the clean surface of a zeolite particle having the electron diffraction pattern of zeolite X (Fig. 4a). On the other hand, we observed a number of small particles with average size of 4.2 nm on the outer surface of Eu(II)X-air (Fig. 4c). The electron diffraction patterns of these particles (area II) revealed the d values of 2.95, 2.43, 1.78, and 1.51 Å, corresponding to (111), (200), (220), and (222) planes of NaCl type EuO (Fig. 4e). We did not observe any electron diffraction pattern of EuO from the inside of the Eu(II)X-air particle (area I), but only that of the zeolite (Fig. 4d). The result indicated the formation of EuO nanocrystals only on the outer surface of Eu(II)X-air. Therefore, the emission below 450 nm of Eu(II)X-air (12 days) was then considered to be the emission from the EuO nanocrystals. The size distribution of the nano-sized EuO particles is also demonstrated in Fig. 4f. The average particle size was 4.2 nm and the range of the size was 2–7 nm, the narrow size distribution is due to the stabilizing effect of the zeolite surface.

We propose a formation mechanism of EuO nanocrystals as shown in Fig. 5. When Eu(II)X is kept in the atmosphere, O_2 rapidly penetrates the cavity of the zeolite X. A molecule of O_2 oxidizes four Eu(II), giving four Eu(III) cations and two O^{2-} anions. Note that an increase of the valence state of Eu(II) to Eu(III) breaks the charge balance between cations and minus charges of zeolite X, so that two Eu(II) cations will be forced out of zeolite X (Step 1). The two Eu(II) cations react with two O^{2-} anions to give EuO nanocrystals on the outer surface of the zeolite X (Step 2).

Magnetic Measurements. According to our previous studies, the spindle-type EuO nanocrystals (av. length of 280 nm and width of 95 nm), which were prepared from liquid ammonia method, showed ferromagnetism at low temperatures, but the photoemission and photo-response magnetism (an increase of magnetization under UV irradiation) were not observed.[22] On the other hand, the photo-emissive EuO nanocrystals prepared (av. diameter of 3.4 nm) by a photochemical reaction of $Eu(NO_3)_3$ did not show ferromagnetism.[21] We were interested in the magnetic properties of EuO specimens having the nano size located at the outer surface of zeolites.

We performed the magnetic measurements of Eu(II)X, Eu(III)X and Eu(II)X-air. The temperature (T) dependences of the magnetization (M) of Eu(II)X and Eu(II)X-air are shown in Fig. 6a and Fig. 6b. We found that both Eu(II)X and Eu(II)X-air were paramagnetic. However, Eu(II)X-air turned into ferromagnetic phase below 70 K (Fig. 6b). The curie point of Eu(II)X-air was the same as that of bulk EuO. According to the magnetic field (H) dependence of magnetization (M), we observed an **S** character-type curve, indicating ferromagnetism of Eu(II)X-air. Eu(II)X-air also revealed an increase of magnetization under irradiation of UV light, as found in the emissive EuO nanocrystals (Fig. 6b). It should be emphasized that EuO nanocrystals formed on the outer surface showed not only strong emission and photo-response magnetism, but also ferromagnetism, which was not observed for the EuO nanocrystals prepared by a photochemical reaction without zeolite. Not only the size of the crystals but also the surface structure of the crystals affected by the surrounding environments should affect their magnetic properties.

Conclusions

Europium(II)-exchanged zeolite X was prepared for the first time by the ion exchange of NaX with Eu(II), which was prepared by a photochemical reaction. Emission spectra and XPS spectra of Eu(II)X indicated that Eu(II) were incorporated in the cavity of zeolite X. When Eu(II)X was exposed to the atmosphere, EuO crystals having the average size of 4.2 nm were formed on the outer surface of zeolite X through the oxidation of Eu(II) in the cavity with oxygen. The EuO nanocrystals located on the outer surface of zeolites showed ferromagnetism at low temperatures. The present work showed that not only the size of the crystals but also the surface structure of the crys-

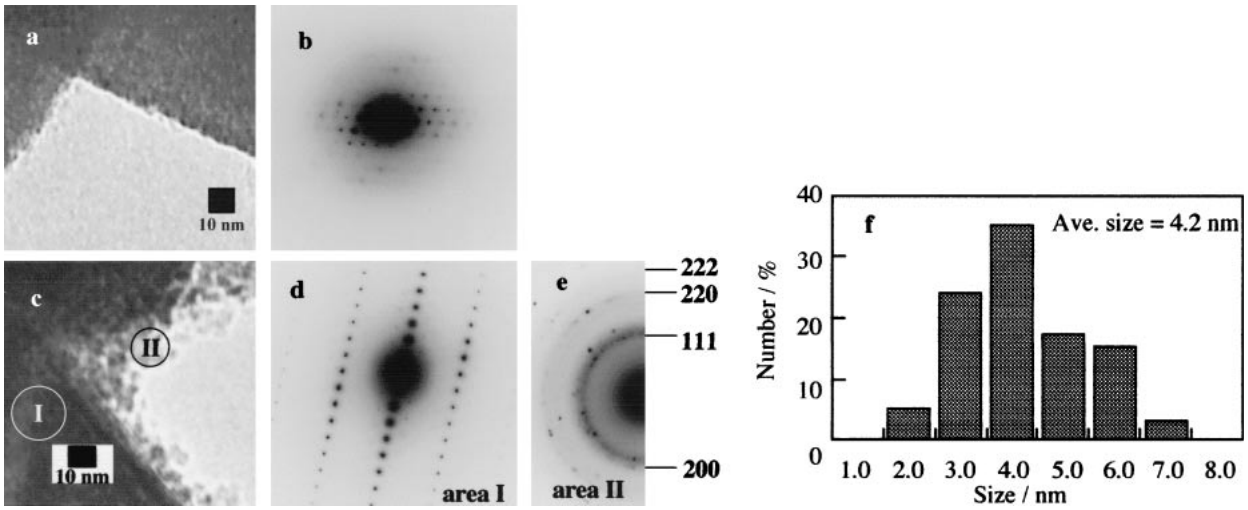

Fig. 4. (a) TEM images of Eu(II)X. (b) Electron diffraction pattern of Eu(II)X nanocrystals. (c) TEM images of Eu(II)X-air. (d) Electron diffraction pattern in area (I) of Eu(II)X-air. (e) Diffraction pattern of area (II) of Eu(II)X-air. (f) Size distribution of the EuO nanocrystals.

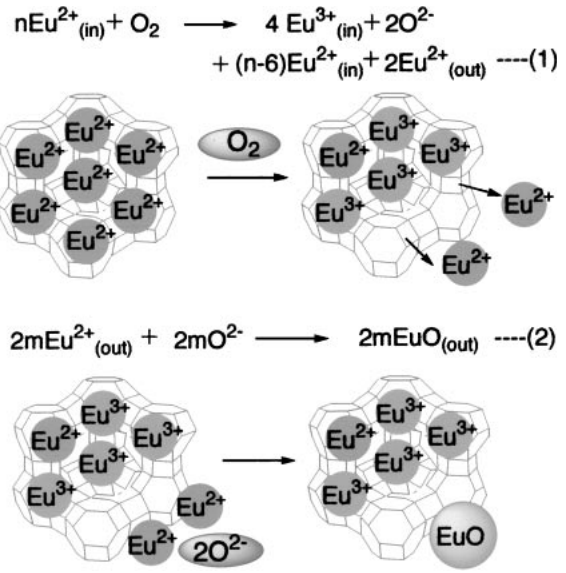

Fig. 5. Postulated reaction mechanism of oxidation of Eu(II)X and formation of EuO nanocrystals ($Eu^{n+}{}_{(in)}$ = a europium ion locating inside the cavity of zeolite X, $Eu^{n+}{}_{(out)}$ = a europium ion on the outer surface of zeolite X).

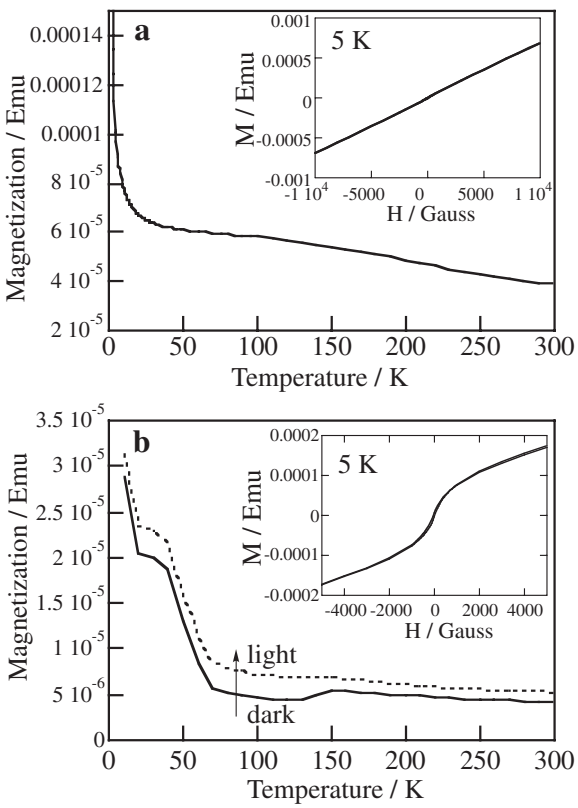

Fig. 6. a) The M/T curve of Eu(II)X and the M/H curve Eu(II)X (inset). b) M/T curves in darkness (dash line) and when irradiated with 254 nm light (solid line), and M/H curves of Eu(II)X-air (b inset).

tals affected by the surrounding environments should affect their magnetic properties. Furthermore, photoemission and photo-response magnetic properties were observed in the EuO nanocrystals presented in this work. The EuO nanocrystals would be promising for luminescent material and optical devices. Especially, Eu(II)X-air having photo-response ferromagnetism is expected to be useful in applications such as photo-assisted isolators and magnetic devices for optical telecommunication systems.[21]

We would like to make grateful acknowledgement to Assistant Professor Hidekazu Tanaka and Mr. Youhei Yamamoto for SQUID measurements. This research is supported by NEDO (New Energy Industrial Technology Development Organization) and Grant-in-Aid for Scientific Research No. 13740397. A part of this work was supported by "Nanotechnology Support Project" of the Ministry of Education, Culture, Sports, Science and Technology (MEXT) Japan, and 21st Century, Center of Excellent Program (COE) for Integrated EcoChemistry.

References

1 G. D. Stucky and J. E. Mac Dougall, *Science*, **247**, 669 (1990).

2 M. E. Davis, *Nature*, **417**, 813 (2002).

3 J. He, D. D. Klug, J. S. Tse, and K. F. Preston, *Chem. Commun.*, **1997**, 1265.

4 J. He, Y. Ba, C. Ratcliffe, J. A. Ripmeester, D. D. Klug, J. S. Tse, and K. F. Preston, *J. Am. Chem. Soc.*, **120**, 10697 (1998).

5 M. Ryo, Y. Wada, T. Okubo, T. Nakazawa, Y. Hasegawa, and S. Yanagida, *J. Mater. Chem.*, **12**, 1748 (2002).

6 Y. Wada, T. Okubo, M. Ryo, T. Nakazawa, Y. Hasegawa, and S. Yanagida, *J. Am. Chem. Soc.*, **122**, 8583 (2000).

7 M. Alvaro, V. Fornes, S. Garcia, H. Garcia, and J. C. Scaiano, *J. Phys. Chem. B*, **102**, 8744 (1998).

8 M. D. Baker, M. M. Olken, and G. A. Ozin, *J. Am. Chem. Soc.*, **110**, 5709 (1988).

9 C. Borgmann, J. Sauer, T. Jüstel, U. Kynast, and F. Schüth, *Adv. Mater.*, **11**, 45 (1999).

10 Y. Nozue, T. Kodaira, and T. Goto, *Phys. Rev. Lett.*, **68**, 3798 (1992).

11 Y. Nozue, T. Kodaira, S. Ohwashi, T. Goto, and T. Osamu, *Phys. Rev. B*, **48**, 12253 (1993).

12 G. Ihlein, F. Schuth, O. Krauss, U. Vietze, and F. Laeri, *Adv. Mater.*, **10**, 1117 (1998).

13 G. Wirnsberger and G. D. Stucky, *Chem. Mater.*, **12**, 2525 (2000).

14 P. Enzel and T. Bein, *Chem. Mater.*, **4**, 819 (1992).

15 T. Kyotani, T. Nagai, S. Inoue, and A. Tomita, *Chem. Mater.*, **13**, 4413 (2001).

16 W. Chen, X. Zhang, and Y. Huang, *Appl. Phys. Lett.*, **76**, 2328 (2000).

17 J. H. Greiner and G. J. Fan, *Appl. Phys. Lett.*, **9**, 27 (1966).

18 K. Tanaka, N. Tatehara, K. Fujita, and K. Hirao, *J. Appl. Phys.*, **89**, 2213 (2001).

19 N. Miura, M. Kawanishi, H. Matsumoto, and R. Nakano, *Jpn. J. Appl. Phys.*, **38**, L1291 (1999).

20 K. Tanaka, K. Fujita, N. Soga, J. Qui, and K. Hirao, *J. Appl. Phys.*, **82**, 840 (1997).

21 Y. Hasegawa, S. Thongchant, Y. Wada, H. Tanaka, T. Kawai, T. Sakata, H. Mori, and Y. Shozo, *Angew. Chem. Int. Ed.*, **42**, 2073 (2002).

22 S. Thongchant, Y. Hasegawa, Y. Wada, and S. Yanagida, *Chem. Lett.*, **2001**, 1274.

23 S. Thongchant, Y. Hasegawa, Y. Wada, and S. Yanagida, *J. Phys. Chem. B*, **107**, 2193 (2003).

24 S. L. Suib, R. P. Zerger, G. D. Stucky, R. M. Emberson, P. G. Debrunner, and L. E. Iton, *Inorg. Chem.*, **19**, 1858 (1980).

25 G. D. Stucky, L. E. Iton, T. Morrison, G. Shenoy, S. Suib, and R. P. Zerger, *J. Mol. Catal.*, **27**, 71 (1984).

26 T. Arakawa, T. Tanaka, G. Adachi, and J. Shiokawa, *J. Chem. Soc., Chem. Commun.*, **1979**, 453.

27 T. Arakawa, T. Tanaka, G. Adachi, and J. Shiokawa, *J. Lumin.*, **20**, 325 (1979).

28 T. Arakawa, T. Tanaka, M. Takakuwa, G. Adachi, and J. Shiokawa, *Mat. Res. Bull.*, **17**, 171 (1982).

29 T. Donohue, *J. Chem. Phys.*, **67**, 5402 (1977).

30 T. Donohue, *Opt. Eng.*, **18**, 181 (1979).

31 M. Kusaba, N. Nakashima, W. Kawamura, Y. Izawa, and C. Yamanaka, *Chem. Phys, Lett.*, **197**, 136 (1992).

32 W. Schneider, C. Laubschat, I. Nowik, and G. Kaindl, *Phys. Rev. B*, **24**, 5422 (1981).

33 R. Vercaemst, D. Poelman, L. Fiermans, R. L. Van Meirhaeghe, W. H. Laflere, and F. Cardon, *J. Electron. Spectrosc. Rel. Phenom.*, **74**, 45 (1995).

34 Y. Uwamino, T. Ishizuka, and H. Yamatera, *J. Electron. Spectrosc. Rel. Phenom.*, **34**, 67 (1984).